

EPR Identification of the Structure of the V_1 Color Center in KCl

F. W. PATTEN AND F. J. KELLER*

U. S. Naval Research Laboratory, Washington, D. C. 20390

(Received 27 June 1969)

EPR spectra have been observed in KCl for a radiation-induced defect center having the same optical and thermal bleaching properties as the center responsible for the V_1 optical-absorption band. The spectra are interpreted as due to an interstitial Cl^0 , or an H center, adjacent to a substitutional cation impurity, most likely Na^+ . The impurity ion is in the $\{100\}$ plane containing the H -center bonding axis and is located nearest the midpoint of the H center. The hyperfine principal axes of the two central Cl nuclei, which are coincident with their bonding axes, are inclined 2.8° and 8.8° from a $\langle 110 \rangle$ direction toward the impurity ion. An analysis of motional effects on the EPR spectra leads to the following values for the activation energy for reorientation: 0.027 eV for the H centers, 0.035 eV for the V_1 center.

I. INTRODUCTION

THE nature of the V_1 optical-absorption band in KCl has been the subject of considerable speculation for many years.¹ Seitz initially proposed² that the center responsible for this band is the antimorph of the F center, i.e., a hole trapped at a cation vacancy. Teegarden and Maurer³ found that V_1 centers and H centers can be reversibly converted into one another by optical and thermal bleaching. Optical bleaching into the V_1 band of a KCl crystal at less than 40°K causes it to disappear and the H band appear; the H band can be made to convert back to the V_1 band by warming the crystal above about 45°K . Känzig and Woodruff⁴ were able to produce the electron paramagnetic resonance (EPR) spectrum of H centers by optically bleaching at 20°K into the V_1 band of crystals which had previously been x-irradiated at 78°K . Since no EPR spectrum had been observed before bleaching, they suggested the V_1 center is diamagnetic and proposed that it is a halogen molecule (Cl_2) occupying an anion site, i.e., an H center that has captured a hole. Yuster⁵ and Kolopus, Delbecq, Schoemaker, and Yuster⁶ reported that the V_1 center in KCl is associated with a Na impurity and suggested that the center is an H center trapped near a Na ion. They showed that the center is paramagnetic by correlating the V_1 optical-absorption band with a one-line isotropic EPR signal.

In this paper we report anisotropic EPR spectra which we interpret as due to an H center located adjacent to a substitutional Na ion. Our analysis indicates a definite position for the impurity with respect to the distorted H center. The thermal and optical behavior of this paramagnetic center is the same as that described above for the optical V_1 band. There-

fore, our data support the proposal of Yuster and of Kolopus *et al.*, and further give a specific model for the V_1 center.

II. EXPERIMENTAL METHODS

Most of the crystals used in this work were grown at this laboratory and were deliberately doped with Na. Crystals with chance Na impurities were purchased from Harshaw and Optovac. Some extremely Na-free crystals were obtained from the Oak Ridge National Laboratory. Sample sizes for EPR experiments were generally about $2 \times 2 \times 10 \text{ mm}^3$.

EPR spectra were measured with a Varian E-3 spectrometer with 100-kHz detection and a rectangular TE_{012} resonant cavity. The samples were suspended within an evacuated double-walled quartz tube (11-mm o.d., 5-mm i.d.) that was inserted in the cavity. Samples were cooled by a flow of cold helium gas through the tube. The sample temperature depended on the helium flow rate, and could be varied from 4 to about 150°K . The interval of best temperature regulation was from 4 to about 50°K . After equilibrium had been attained within this interval, the temperature varied less than 0.5°K over a time period of about 5 min. The temperature gradient along the sample was less than $0.5^\circ\text{K}/\text{cm}$. This cryogenic arrangement will be the subject of a subsequent publication.⁷

The sample was fastened to the end of a quartz tube (nominally 3 mm o.d., 2 mm i.d.) with vacuum grease and suspended in the stream of the coolant. The tube contained a copper-constantan thermocouple whose test junction was separated from the sample by less than 1 mm of vacuum grease. The thermocouple was calibrated at the boiling points of liquid helium and liquid nitrogen.

The samples were either x-irradiated (45 kV, 35 mA) or electron-irradiated with a Van de Graaff accelerator (2 MeV, $10 \mu\text{A}$). The x rays were filtered through a thin Be window, about 1 mm of quartz, and a few mm of liquid nitrogen. During the x irradiation, the samples were immersed in liquid nitrogen, while during the

* Permanent address: Clemson University, Clemson, S. C.

¹ J. H. Schulman and W. D. Compton, *Color Centers in Solids* (The Macmillan Co., New York, 1962).² F. Seitz, *Phys. Rev.* **79**, 529 (1950); *Rev. Mod. Phys.* **26**, 7 (1954).³ K. Teegarden and R. J. Maurer, *Z. Physik* **138**, 284 (1954).⁴ W. Känzig and T. O. Woodruff, *J. Phys. Chem. Solids* **9**, 70 (1958).⁵ P. H. Yuster, invited paper, Washington APS Meeting, 1967 (unpublished).⁶ J. L. Kolopus, C. J. Delbecq, D. Schoemaker, and P. H. Yuster, *Bull. Am. Phys. Soc.* **12**, 467 (1967).⁷ F. W. Patten and F. J. Keller (unpublished).

electron irradiation the samples were cooled by a stream of cold ($\sim 80^\circ\text{K}$) nitrogen gas.

Optical bleaching was performed with a Bausch and Lomb mercury vapor lamp in conjunction with one or more Corning filters. Computed EPR spectra were obtained using a Control Data Corporation 3800 computer and a Calcomp graphical plotter. Chemical analyses of the samples for sodium concentration were performed at this laboratory using the technique of flame emission spectroscopy.

III. RESULTS

A. EPR Spectra

Single crystals of KCl containing up to 600 ppm of Na were x-irradiated from 4 to 20 h or exposed to a Van de Graaff electron beam from 20 to 60 min with the sample maintained at liquid-nitrogen temperature (LNT). Samples were transferred, without significantly raising the temperature, to the variable temperature insert in the resonant cavity of the EPR spectrometer. The intense EPR spectrum due to V_K centers⁸ at LNT was used to orient the crystals with an estimated accuracy of $\pm 0.5^\circ$, since the principal axis coincident with the internuclear axis of the V_K center is known to be exactly aligned along the $\langle 110 \rangle$ crystal directions. V_K centers were then eliminated by optically bleaching the crystal with an unfiltered tungsten lamp. It is believed that the bleaching light releases trapped electrons that are attracted to the positively charged V_K centers, resulting in their mutual annihilation. Upon lowering the crystal temperature, a new EPR spectrum whose amplitude was strongly temperature-dependent appeared within the interval 25–45°K. The spectrum was unaffected by the bleaching light, implying that the paramagnetic centers giving rise to the spectrum were either neutral or negatively charged.

A typical spectrum is shown in Fig. 1(a) for the case of the applied magnetic field oriented approximately along a $\langle 110 \rangle$ direction, and a crystal temperature of 35°K. For comparison, an H -center spectrum, for the same field orientation but for a crystal temperature of 25°K, is shown in Fig. 1(b). This color center is known⁴ to have a structure as shown in Fig. 2, and consists of a Cl_2^- molecule ion in a $\langle 110 \rangle$ orientation at the site of a Cl^- vacancy. Since there is one electron missing from a closed molecular orbital shell, this is viewed as a hole-type color center. There is additional measurable hyperfine interaction of the hole with the two nearest anions along the internuclear axis of the center, and, consequently, some degree of covalent bonding with them. Alternatively, the center may be viewed simply as an interstitial Cl atom.

The spectra in Fig. 1 display a strong similarity to one another, both having a set of seven groups of hyperfine lines with about the same width and spacing

between groups in each spectrum. [The additional transitions bordering the outer groups in each spectrum belong to FCl^- , mixed V_K centers.⁹ They are $\langle 111 \rangle$ -oriented centers, and the doublet splittings observed in the figure indicate a small misorientation within the $\langle 110 \rangle$ plane of this particular sample.] The hyperfine structure within corresponding groups of Figs. 1(a) and 1(b) is considerably different, however. In general, the ESR hyperfine structure is due to transitions between the two-spin states of the unpaired electron, $\Delta M_S = \pm 1$, while interacting nuclear magnetic dipoles maintain their relative orientations with respect to the applied magnetic fields, $\Delta m_I = 0$. Hyperfine transitions, grouped symmetrically about the center of the spectrum, are labeled by their nuclear magnetic quantum numbers. The two central Cl nuclei, of spin $I = \frac{3}{2}$, in an H center have the largest hyperfine interaction energy. Their equivalent interaction with the unpaired electron produces seven hyperfine lines, each split into sets of lines because Cl has two naturally occurring isotopes with different magnetic moments. The more weakly interacting two outer Cl^- nuclei in the H center further split the hyperfine lines within each set. It is reasonable to expect that small changes in the hyperfine interactions would maintain the seven sets of lines but change the structure within each set. We are led to interpret the spectrum of Fig. 1(a) as due to an H -like center, perturbed by some kind of nearby lattice imperfection. We shall call this configuration a V_1 center, and evidence will be presented later to show that it is responsible for the V_1 optical-absorption band.

B. Model of V_1 Center

The anisotropy of the hyperfine structure as a function of magnetic field orientation within both (100) and (110) planes showed that the V_1 center molecular axis lies approximately along a $\langle 110 \rangle$ direction. However, for small-angle rotations of the field direction in the (100) plane, the spectrum width was observed to maximize at about $\pm 5^\circ$ from $\langle 110 \rangle$; for a small-angle (110) rotation, the maximum occurred exactly along $\langle 110 \rangle$. Thus the V_1 molecular axis, as represented roughly by the direction of the largest hyperfine splitting, deviates somewhat from $\langle 110 \rangle$ only in a $\{100\}$ plane. This plane must also contain the lattice imperfection.

Of the different types of lattice imperfections which might cause the stabilization of the H center at elevated temperatures, a substitutional cation impurity in a neighboring site was considered most likely. Since Na is a common impurity in this material, it was the primary suspect. Several samples, from sources previously specified, with varying amounts of Na impurity were examined for V_1 -center concentration. Sample sizes, radiation exposure, and other experimental conditions were nearly identical in all cases. The results,

⁸ T. G. Castner and W. Känzig, J. Phys. Chem. Solids 3, 178 (1957).

⁹ D. Schoemaker, Phys. Rev. 149, 693 (1966).

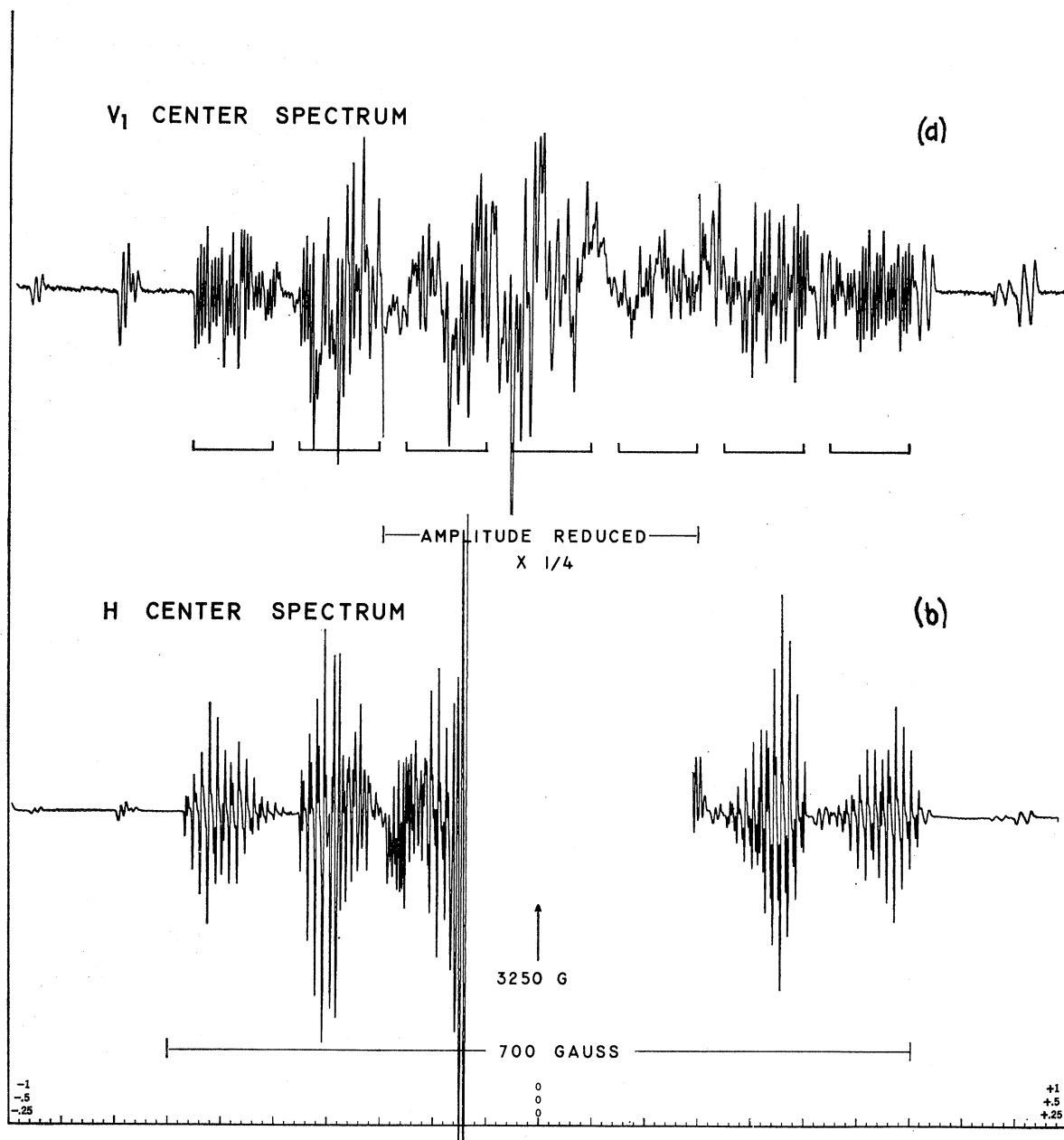


FIG. 1. (a) EPR spectrum (dx''/dH) observed in KCl:NaCl single crystals after irradiation at 80°K . $T=35^\circ\text{K}$ and \mathbf{H} approximately along a $\langle 110 \rangle$. (b) Comparison with the H -center spectrum in the same crystal with the same orientation. $T=25^\circ\text{K}$.

shown in Fig. 3, show that the concentration of V_1 centers is a monotonically increasing function of Na impurity.

A model of the V_1 center based on these observations is given in Fig. 4. The different ionic sizes are shown to their proper proportion in the figure. As is seen, the neighboring cation impurity of smaller ionic radius can pictorially explain the "tipping" of the molecular axis. The data do not indicate the existence of the "symmetric" nearest-neighbor position for the impurity Na

ion, above (or below) the midpoint of the central Cl_2^- and out of the plane of Fig. 4. However, it is likely that the EPR spectrum for this configuration would not be distinguishable from that of the H center. Since all H -like-center spectra can be thermally annealed at lower temperatures than V_1 -center spectra (see Sec. III D), we conclude that the center with the Na^+ impurity in the "symmetric" position is less stable energetically than the configuration of Fig. 4.

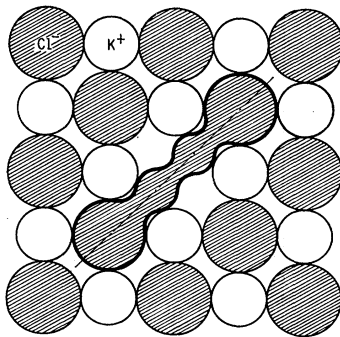
C. Spin Hamiltonian Analysis

Since the EPR spectra exhibit orthorhombic symmetry, the following spin Hamiltonian, in conventional notation, was used to analyze the V_1 -center EPR spectra:

$$\mathcal{H}/g_0\beta = (1/g_0)(g_z H_z S_z + g_x H_x S_x + g_y H_y S_y) + \sum_{i=1}^4 (A_{i,z} S_z I_{i,z} + A_{i,x} S_x I_{i,x} + A_{i,y} S_y I_{i,y}). \quad (1)$$

The summation, with index i , over the Cl hyperfine interactions is such that $i=1, 2$ represents the central two atoms, and $i=3, 4$ represents the outer atoms. Additional terms in Eq. (1), such as the nuclear Zeeman and quadrupole interaction terms, were considered of negligible effect within the observational accuracy. Bleaney¹⁰ has derived a formula for the angular dependence of the $\Delta M_S = \pm 1$, $\Delta m_I = 0$ transitions for an axial spin Hamiltonian for a single atom, to second order in the hyperfine interaction. His formula can be used in the present situation for the Hamiltonian of Eq. (1) for rotations of the applied magnetic field \mathbf{H} up to about $\pm 45^\circ$ from $\langle 110 \rangle$ within the (100) and (110) planes.

The anisotropy of the spectra indicate that there are two magnetically distinct centers associated with each of the lattice $\langle 110 \rangle$ directions, a total of twelve inequivalent sites for an arbitrary orientation of \mathbf{H} . This is evident from the model of the V_1 center in Fig. 4. Because of the overlapping of spectra from nearly equivalent centers, it was not possible to follow individual transitions beyond about $\pm 35^\circ$ from $\langle 110 \rangle$ in either plane. The most easily interpretable spectrum is obtained for \mathbf{H} along a $\langle 110 \rangle$. The two centers associated with this direction are then magnetically equivalent, and their spectrum [indicated by brackets in Fig. 1(a)] is largely unobscured by the more compressed spectra from centers in other sites. We obtained the following hyperfine constants and g factor for this



H CENTER

FIG. 2. Model of the H center in KCl (Ref. 4).

¹⁰ B. Bleaney, Phil. Mag, 42, 441 (1951).

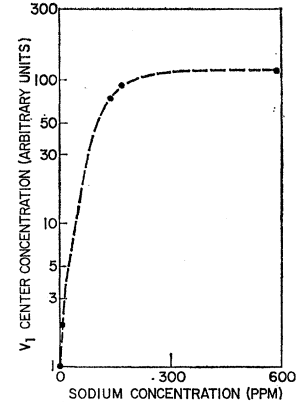
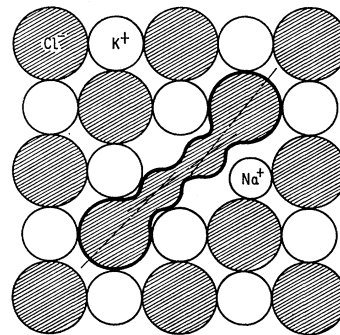


FIG. 3. V_1 -center concentration in KCl as a function of Na concentration.

field orientation: $A_1=109.1$ G, $A_2=100.3$ G, $A_3=13.6$ G, $A_4=3.0$ G, $g=2.0020$. In order to extract these parameters accurately from the data, a computer simulation of the recorded spectrum was performed. First derivatives of Gaussian functions of given half-width at the computer field positions for all first-order transitions were summed over the entire field scan. A comparison of recorded and computer spectra is shown in detail in Fig. 5 for the high-field portion of the $\mathbf{H} \parallel [110]$ spectrum. The occasional dissimilarities in the amplitudes of corresponding transitions were found to be due to overlapping transitions from FCl^- or residual Cl_2^- centers.

The linewidth of the V_1 center EPR transitions is 1.8 G, compared with the H -center linewidth of 0.8 G. A major portion of the linewidth of the H center is attributed to unresolved hyperfine structure due to interactions with neighboring nuclei.⁴ If we assume that the increased linewidth of the V_1 -center transitions is due mainly to interaction with the Na nucleus ($I=\frac{3}{2}$), then the Na hyperfine constant is estimated to be ~ 0.4 G.

In Fig. 6 are shown the variations of the hyperfine constants A_1 and A_2 for the inner Cl nuclei and the g factor for rotations of \mathbf{H} within the (100) plane up to $\pm 15^\circ$ about a $\langle 110 \rangle$. The curves which have been



V_1 CENTER

FIG. 4. Model of the V_1 center in KCl.

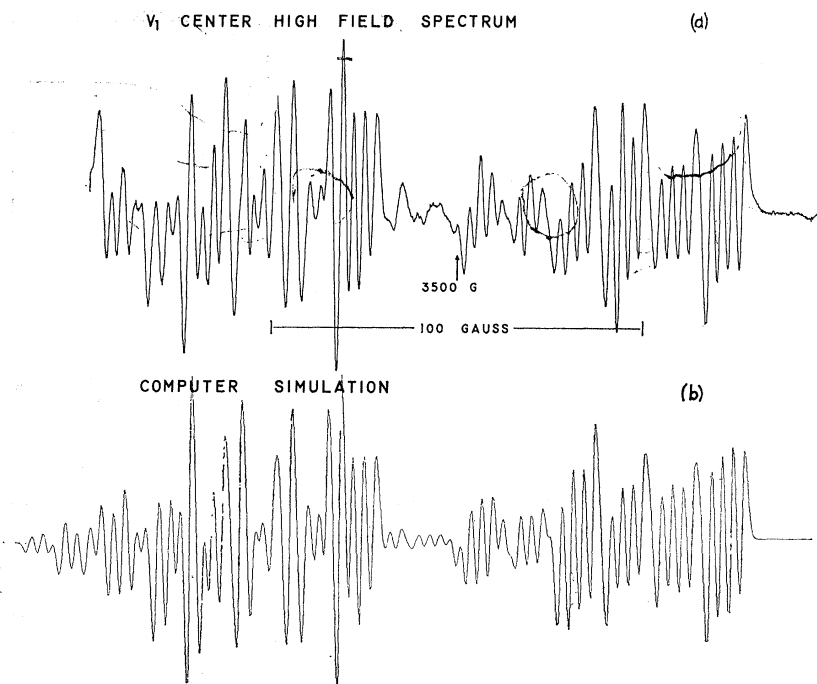


FIG. 5. (a) High-field portion of the V_1 -center EPR spectrum for $\mathbf{H} \parallel \langle 110 \rangle$. (b) Computer simulation of this portion of the spectrum, using hyperfine constants given in the text.

fitted to the data points are the expected forms for the angular variation of the hyperfine constants and g factor:

$$A_i(\theta) \cong A_{i,0} \cos(|\theta| - |\theta_i|) \quad (\text{for small } \theta),$$

$$g(\theta) = [g_z^2 \cos^2(|\theta| - |\theta_0|) + g_x^2 \sin^2(|\theta| - |\theta_0|)]^{1/2}. \quad (2)$$

The quantities θ_0 and θ_i are the angular deviations from the $\langle 110 \rangle$ of the principal axes corresponding to g_z and

$A_{i,z}$, respectively. Application of Eqs. (2) requires an *a priori* knowledge of the spin Hamiltonian constants (Table I), though approximate values may be assumed initially. The following values were found: $\theta_0 = 5.6^\circ$, $\theta_1 = 2.8^\circ$, $\theta_2 = 8.8^\circ$, each with an estimated error of $\pm 0.5^\circ$. The relatively small magnitude of the hyperfine constants for the outer Cl nuclei precluded a determination of any deviation of their principal axes from $\langle 110 \rangle$. In fact, the constancy of these parameters over the angular interval was assumed in calculating the variations of A_1 and A_2 .

Variations of the hyperfine constants and g factor also were studied for rotations of \mathbf{H} within the $\langle 110 \rangle$ plane about a $\langle 110 \rangle$. In this case there were observed no angular displacements of the principal axes from $\langle 110 \rangle$. Figure 7 illustrates the relative orientations of the principal-axis systems required to diagonalize the hyperfine and g tensors. The hyperfine principal axes for the outer Cl nuclei $z_{3,4}$ are taken to lie along $\langle 110 \rangle$.

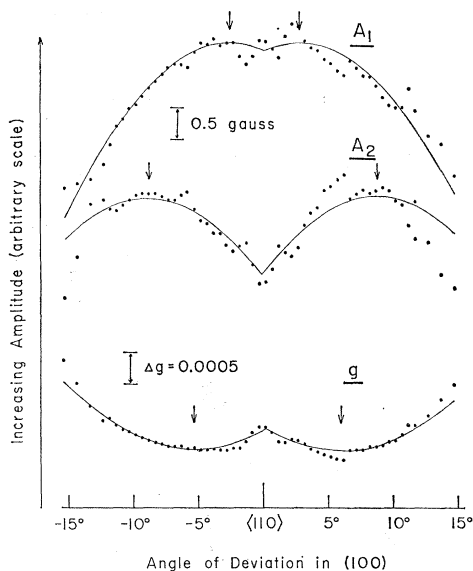


FIG. 6. Dependences of the amplitude of A_1 , A_2 , and g on field orientation within $\langle 100 \rangle$, on either side of a $\langle 110 \rangle$. Positions of the extrema are indicated.

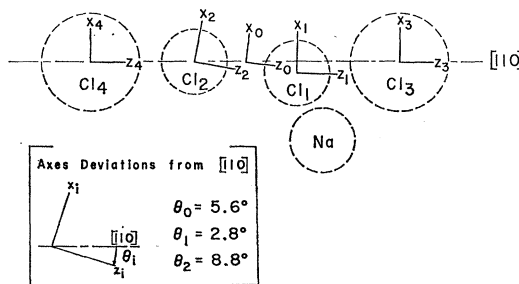


FIG. 7. Relative orientations of principal-axis systems of the hyperfine tensors and g factor for the V_1 center.

The directions of the x_i and y_i principal axes are obvious from the local symmetry.

It seems reasonable, from physical intuition, that θ_0 and θ_i must all have an associated positive sign, as defined in the insert of Fig. 7; that is, z_0 , z_1 , and z_2 must all be inclined from $\langle 110 \rangle$ toward the Na impurity, as shown in the figure. This conclusion may be reached in a more direct manner since it is possible to establish a relation between the relative orientations of the three principal axes, for small deviations from $\langle 110 \rangle$. It is shown in the Appendix that

$$(\theta_0 - \theta_1) / (\theta_2 - \theta_1) \cong \beta_2 \nu_2 / (\beta_1 \nu_1 + \beta_2 \nu_2), \quad (3)$$

where β_1 , β_2 and ν_1 , ν_2 are atomic orbital coefficients in the ground- and excited-state molecular orbital wave functions [Eq. (6)]. Since the contributions from atoms 1 and 2 to the molecular orbitals must be nearly equivalent, we may take $\beta_1 = \beta_2$ and $\nu_1 = \nu_2$, and find

$$(\theta_0 - \theta_1) = \frac{1}{2}(\theta_2 - \theta_1). \quad (4)$$

Therefore, the z_0 axis is expected to be directed midway between z_1 and z_2 . The experimental values of θ_0 , θ_1 , and θ_2 substantiate this very well, only if all are taken to have the same sign; the obvious choice of sign is such that z_0 , z_1 , and z_2 are inclined from $\langle 110 \rangle$ on the side of the impurity. Further, the direction of z_0 is very nearly that of the internuclear axis for the central Cl atoms 1 and 2.

The ordering of the Cl nuclei relative to the Na impurity was determined in the following way. The fact that the hole, mainly located on the Cl_4^{-3} molecule, interacts significantly with the Na nucleus indicates that it is a source of the shift of values for the constants from those of the H center. Since Na has a greater ionization potential than the K it displaced, it is likely to increase the hole density, and hence the values of the hyperfine constants, on the nuclei in its vicinity. Guided by the unperturbed values for the H center (Table I), we have numbered the nuclei in the order of decreasing values of their hyperfine constants.

The principal values of the spin Hamiltonian tensors for the V_1 center are given in Table I. Also shown, for comparison, are the corresponding values for the H center. It is seen that the hyperfine principal values for the two nuclei nearest the Na^+ impurity have increased in magnitude, while the values for the remaining two nuclei have decreased. Also, the perpendicular elements of the g tensor are more dissimilar than those for the H center, indicating a greater departure from axial symmetry. The significance of these quantities has been discussed adequately for the case of the H center,⁴ and the differences encountered for the V_1 center are not great enough for further elaboration. In general, the unpaired electron (or hole) lies in a molecular orbital principally composed of atomic $3p$ orbitals on nuclei 1 and 2. The directions of these orbitals, coincident with the corresponding hyperfine principal-

TABLE I. Spin Hamiltonian parameters for the V_1 center compared with those for the H center.

Tensor components (G)	V_1 center	H center ^a
$A_{1,z}(\text{Cl}^{35})$	109.2 ± 0.2	109
$A_{1,x}, A_{1,y}(\text{Cl}^{35})$	~ 0	~ 0
$A_{2,z}(\text{Cl}^{35})$	101.6 ± 0.2	109
$A_{2,x}, A_{2,y}(\text{Cl}^{35})$	~ 0	~ 0
$A_{3,z}(\text{Cl}^{35})$	13.6 ± 0.2	7.3
$A_{3,x}, A_{3,y}(\text{Cl}^{35})$	~ 3	2.8
$A_{4,z}(\text{Cl}^{35})$	3.0 ± 0.2	7.3
$A_{4,x}, A_{4,y}(\text{Cl}^{35})$	~ 1	2.8
g_x	2.0017 ± 0.0001	2.0023
g_y	2.038 ± 0.001	2.0227
g_z	2.033 ± 0.001	2.0219

^a Reference 4.

axes directions, deviate somewhat from $\langle 110 \rangle$ toward the Na^+ impurity.

D. Optical and Thermal Bleaching Characteristics

In this section we shall show that there is a correspondence between the optical and thermal bleaching properties of the paramagnetic configuration which we have labeled a V_1 center and those of the center responsible for the V_1 optical-absorption band in this material.

It is well known from optical-absorption measurements that there exists a close relationship between the V_1 and H bands at 365 and 336 nm, respectively, in KCl.^{3,11} Thus, when a crystal is x-rayed below 40°K, the H band is produced. This may be eliminated and the V_1 band formed by warming the crystal above about 45°K but below 110°K. If the crystal is cooled again below 40°K and illuminated in the region of 365 nm, the V_1 band bleaches and the H band is regenerated. The cycle may be repeated, with consequent loss of a fraction of the optical density within each band. Since an optical transition of the H center, as identified by EPR, has been shown to give rise to the H band,¹² we may demonstrate a correspondence between the V_1 band and the V_1 center by repeating for the case of the H -center and V_1 -center EPR spectra the optical conversion-regeneration cycle described above.

Crystals at 35°K containing V_1 centers were bleached in the V_1 band at 365 nm with a mercury lamp and appropriate filters. The EPR spectrum due to the V_1 center was observed to decay as a function of bleaching time, and a new spectrum, identified as that of the H center, emerged. Data for a typical crystal, separately normalized for each spectrum, are shown in Fig. 8. (Since the EPR amplitudes for the H center and V_1

¹¹ W. H. Duerig and J. J. Markham, Phys. Rev. **88**, 1043 (1952).

¹² C. J. Delbecq, J. L. Kolopus, E. L. Yasaitis, and P. H. Yuster, Phys. Rev. **154**, 866 (1967).

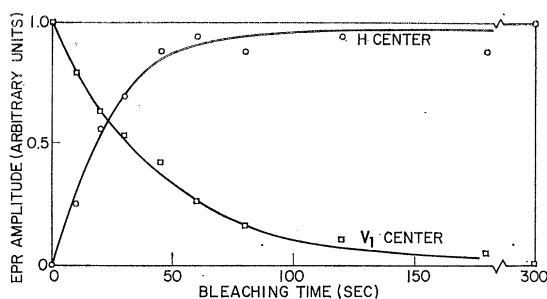


Fig. 8. Conversion of V_1 centers to H centers by optical bleaching at 365 nm.

center were strongly temperature-dependent, each was observed separately at its optimum temperature of 25 and 35°K, respectively; temperature deviations sustained during these alternations produced some scatter in the data.) When the crystals were warmed to about 50°K, the H -center spectrum diminished and the V_1 -center spectrum reappeared, as a function of thermal-annealing time. The entire procedure typically resulted in a loss of about 40% of the initial V_1 -center population. Since the V_1 -center- H -center conversion-regeneration cycle is believed to be the result of motion of the interstitial Cl_0 , the loss is attributed to the recombination of interstitial Cl_0 atoms with F -center electrons.

In order to compare the thermal stability of the V_1 center with that of the V_1 band, pulsed thermal-annealing experiments were carried out. Samples containing V_1 centers were warmed rapidly to a desired annealing temperature, held for ten seconds at this temperature, and cooled again to 35°K for measurement of the EPR spectrum. A plot of EPR amplitude as a function of annealing temperature is given in Fig. 9 for the temperature region in which the centers decayed. Also shown are data of Delbecq, Smaller, and Yuster¹³ from similar measurements performed on the V_1 band; however, in their measurements, the annealing temperature was held for 2 min. The effect of using shorter

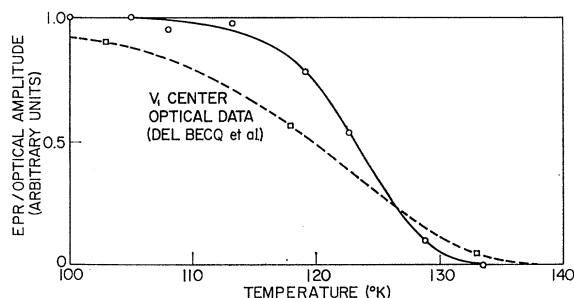


Fig. 9. Comparison of V_1 -center EPR amplitude (solid curve) with V_1 -band optical-absorption amplitude (dashed curve) after pulsed thermal annealing, as a function of annealing temperature. Annealing time was 10 sec for EPR measurements, 2 min for optical-absorption measurements (Delbecq *et al.*, Ref. 13).

¹³ C. J. Delbecq, B. Smaller, and P. H. Yuster, *Phys. Rev.* **111**, 1235 (1958).

annealing times is to cause a decay curve to have a steeper decline and to shift its point of a maximum descent toward higher temperatures. Thus the maximum decay rates for the optical-absorption band and EPR amplitudes of about 118 and 123°K, respectively, compare satisfactorily.

E. Temperature Dependence of EPR

Delbecq *et al.*,¹² in studying the dichroism of the H center at low temperatures, found its disorientation temperature to be 10.9°K. Disorientation presumably occurs by a process in which the weak bonds between the outer nuclei (3 and 4) and the central nuclei (1 and 2) are broken; they are then reformed with another pair of neighboring nuclei after rotation of the central pair. The reorientational motion has no effect on the EPR spectra until the correlation time for reorientation τ is of the order of the linewidth. When this condition is met, line broadening occurs and a consequent decrease of peak amplitudes. Further increasing τ , by increasing the temperature, leads to an EPR spectrum which is the result of averaging the g tensor and hyperfine tensor principal values.

The effect of line broadening on the EPR amplitudes of the V_1 center and H center is seen in Fig. 10. Extrema for the slopes of the curves in the line-broadening regions occur at (38 ± 3) °K for the V_1 center and at (27 ± 3) °K for the H center. The reduction of EPR amplitudes in the low-temperature regions of the curves was due to power saturation of the resonance absorption. As the temperature is raised to about 70°K, a single broad absorption, which is probably the spectrum of the completely motionally averaged V_1 center, appears in the EPR spectra.¹⁴

It may be seen from Fig. 4 that reorientation can take place by rotation of the central Cl_2^- only to the four $\langle 110 \rangle$ -associated sites which are in $\{100\}$ containing the Na^+ impurity site. We would expect one type of reorientational motion of the V_1 center to be similar to that for the H center but, because of the constraint imposed by the presence of the sodium in its configuration, somewhat more restricted. Another type of

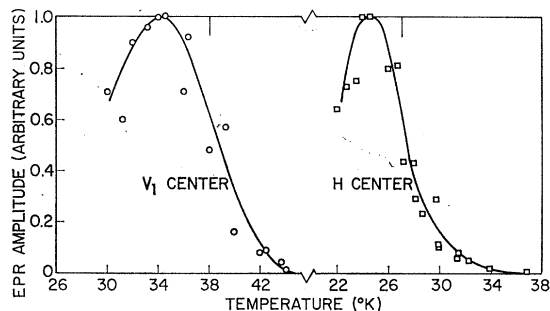


Fig. 10. Amplitudes of V_1 -center and H -center EPR transitions as a function of temperature (different temperature scales).

¹⁴ Previously observed by Kolopus *et al.*, Ref. 6.

reorientational motion of the V_1 center can occur by a translation of the interstitial Cl^0 along the bond direction a distance of (lattice constant)/ $\sqrt{2}$. The central Cl_2^- of the V_1 center in the new location is then tipped toward the Na^+ at an angle opposite to its former sense. Line-broadening effects due to this motion would be very small, and, in fact, there would be no effect with $\mathbf{H} \parallel \langle 110 \rangle$ for the two centers associated with the field direction. No part of the experimentally observed line broadening could be attributed to this type of reorientational motion.

Gutowsky and Saika¹⁵ have developed a theory for magnetic-resonance-spectrum changes during motional averaging. Applying their theory to this problem in the region of initial line broadening, we obtain the following values for the correlation time for reorientation: (1) V_1 center at 38°K, $\tau = 2.4 \times 10^{-8}$ sec; (2) H center at 27°K, $\tau = 5.9 \times 10^{-8}$ sec. If, in addition, we take $\tau = 1$ sec for the H center at $T = 11^\circ\text{K}$,¹² and assume the validity of the Arrhenius relation

$$1/\tau = \nu_0 e^{-E/kT}, \quad (5)$$

we find the following for the activation energy and frequency factor of the H center: $E(H \text{ center}) = 0.027 \pm 0.004$ eV, $\nu_0 = 1.6 \times 10^{12}$ sec⁻¹. Since no additional datum point exists for the V_1 center, we use the same frequency factor and obtain $E(V_1 \text{ center}) = 0.035 \pm 0.005$ eV. From this result, we estimate the disorientation temperature of the V_1 center to be $(15 \pm 2)^\circ\text{K}$.

IV. CONCLUSION

Low-temperature irradiation of KCl crystals containing ~ 100 ppm Na results in the formation of a paramagnetic center that is closely related to the H center. Analysis of the EPR spectra shows that the configuration is an H center perturbed by a defect on one of the four equivalent cation sites closest to the midpoint of the H center and in the same (100) plane as the H center. Since the concentration of these centers is a monotonically increasing function of Na concentration, it is likely that the perturbing defect is a substitutional Na impurity ion. The optical and thermal bleaching properties of the centers are the same as those previously reported for the V_1 optical-absorption band. Therefore, we conclude that the V_1 optical-absorption band is due to the configuration described above, consisting of an H center adjacent to a substitutional Na^+ impurity.

ACKNOWLEDGMENTS

The authors wish to express their gratitude to M. N. Kabler and C. C. Klick for stimulating advice, and to I. Schneider for supplying some of the crystals.

¹⁵ H. S. Gutowsky and A. Saika, J. Chem. Phys. **21**, 1688 (1953).

APPENDIX

We shall calculate the shift θ_0 from $\langle 110 \rangle$ of the g_z principal axis z_0 as a function of corresponding shifts θ_1 and θ_2 of the principal axes of the hyperfine tensors for the two central chlorines of the V_1 center. All effects due to the outer chlorines 3 and 4 are neglected. Essentially, the calculation is an extension of that of Inui, Harasawa, and Obata¹⁶ for the g values of the V_K center (Cl_2^-). Ground- and excited-state molecular orbital wave functions Φ_0 and $\Phi_{x,y}$, respectively, are constructed from linear combinations of s and $3p$ atomic orbitals along the principal axes directions (Fig. 7):

$$\begin{aligned} \Phi_0 &= \alpha_1 S_1 + \beta_1 P_{z_1} - \alpha_2 S_2 + \beta_2 P_{z_2}, \\ \Phi_x &= \mu_1 P_{x_1} + \mu_2 P_{x_2}, \\ \Phi_y &= \nu_1 P_{y_1} + \nu_2 P_{y_2}. \end{aligned} \quad (6)$$

It is assumed that π -antibonding excited-state orbitals are of little importance in the ensuing calculation. Taking only the spin-orbit coupling as a perturbation mixing ground and excited states, the modified ground-state functions are calculated to be

$$\begin{aligned} |+\rangle &= N^{-1}(|0, \frac{1}{2}\rangle + \delta|x, -\frac{1}{2}\rangle + i\epsilon|y, -\frac{1}{2}\rangle), \\ |-\rangle &= N^{-1}(|0, -\frac{1}{2}\rangle - \delta|x, \frac{1}{2}\rangle + i\epsilon|y, \frac{1}{2}\rangle), \end{aligned} \quad (7)$$

where

$$\begin{aligned} \delta &= \lambda(\mu_1\beta_1 + \mu_2\beta_2)/2\Delta_x, \\ \epsilon &= \lambda(\nu_1\beta_1 + \nu_2\beta_2)/2\Delta_y, \\ N^2 &= 1 + \delta^2 + \epsilon^2. \end{aligned} \quad (8)$$

Here, λ is the spin-orbit coupling constant for a chlorine $3p$ electron, and $\Delta_{x,y}$ are the energy differences between the ground and excited states. In solving the secular equation for the interaction Hamiltonian, $\beta(\mathbf{L} + g_0\mathbf{S}) \cdot \mathbf{H}$, projections of the orbital angular momentum operator must be taken onto the principal axis systems of chlorines 1 and 2. Proceeding in the usual manner, the g -tensor component along the z_0 axis is obtained to second order in λ/Δ :

$$g_z \cong g_0 [1 - 2(\delta^2 + \epsilon^2) + K + \frac{1}{2}L^2], \quad (9)$$

where

$$\begin{aligned} K &= 2\delta\epsilon[\mu_1\nu_1 \cos(\theta_0 - \theta_1) + \mu_2\nu_2 \cos(\theta_0 - \theta_2)], \\ L &= 2\epsilon[\beta_1\nu_1 \sin(\theta_0 - \theta_1) + \beta_2\nu_2 \sin(\theta_0 - \theta_2)]. \end{aligned} \quad (10)$$

The orientation of the z_0 axis is found by minimizing g_z with respect to θ_0 . The resulting relation between the orientations of the three principal axes is

$$(\theta_0 - \theta_1)/(\theta_2 - \theta_1) \cong \beta_2\nu_2/(\beta_1\nu_1 + \beta_2\nu_2). \quad (11)$$

¹⁶ T. Inui, S. Harasawa, and Y. Obata, J. Phys. Soc. Japan **11**, 612 (1956).